

## Solvation of Ions in Hydrophilic Layer of Polyoxyethylated Nonionic Micelle. Cooperative Approach by Electrophoresis and Ion-Transfer Voltammetry

Takumi Ohki, Makoto Harada, and Tetsuo Okada\*

Department of Chemistry, Tokyo Institute of Technology, Meguro-ku, Tokyo 152-8551, Japan

Received: April 24, 2006; In Final Form: June 10, 2006

Electrophoretic measurements of micellar mobility have revealed that polyoxyethylated nonionic surfactant micelles have negative  $\zeta$  potential in various electrolytes, indicating that the partition of anions into the micelle dominates the entire electrolyte partition and the induced surface potential of the micelle. Although an excess of a negative charge is thus revealed in the micelle, it is uncertain whether anions are preferably solvated in the micelles or cations are expelled from the micelles. To determine the solvation energies of single ions in the hydrophilic layer of the micelle, we have performed ion transfer voltammetric measurements at microinterfaces between nitrobenzene and aqueous tetraethyleneglycol solution, which acts as a model for the palisade layer of the micelles. The cooperative utilization of these different methods has allowed us to determine the Gibbs free energy of transfer of a single ion without an extrathermodynamic assumption. On the basis of the resulting values, the partition of ions and the  $\zeta$  potential induced by the imbalance of anionic and cationic partition have been quantitatively explained.

Molecular structures and dynamics in various confined spaces have received great interest in fundamental and practical branches of chemistry. Recent developments of the materials with controlled nanopores, such as carbon nanotubes,<sup>1,2</sup> MCM-41,<sup>3,4</sup> and zeolites and its families,<sup>5–8</sup> have facilitated the application of various spectroscopic methods to nanospaces to probe the molecular properties therein. Such studies, for example, have revealed the structures and dynamics of water in restricted spaces and have indicated that the walls surrounding the space play a key role.<sup>1–8</sup> The effect of walls obviously becomes more important as the size of the space decreases. Thus, in a confined space, the solvation of molecules and, in turn, their reactivity should be different from that in bulk solvents. Unusual solvation structures of ions have been revealed, for example, by X-ray absorption fine structure.<sup>9</sup>

Micelles and Langmuir monolayers also provide confined spaces in contact with soft and dynamic interfaces.<sup>10–19</sup> These association molecular aggregates are of industrial and biological importance as well as of fundamental interest. A number of useful methods, including thermodynamic, electrochemical, spectroscopic, and computational approaches have been exploited to study the nanospaces<sup>10–16</sup> or nanointerfaces formed by amphiphilic molecules.<sup>17–23</sup> Electrostatic interaction primarily governs the interaction occurring at the interfaces involving ionic amphiphilic molecules and also influences the ionic distribution in a solution near the interface. Ionic solvation also differs at charged interfaces and is often an essential factor determining recognition of ions therein.<sup>16,17</sup> However, it is obvious that an effect of solvation should be more crucial for determination of ionic behavior at uncharged interfaces.

Polyoxyethylene (POE) has been used in various surfactants as hydrophilic moieties, in conductive polymers, and as ionophores because of its capability of complexation with hard cations, miscibility with various solvents, interfacial properties,

and facile preparation of compounds with a wide variety of chain lengths.<sup>21–26</sup> Although the complexation of POE with cations has been addressed in many instances, it is known that this ability is much lower than that of crown ethers.<sup>26</sup> In particular, its complexation is extremely weak in aqueous solutions because of the high solvation capability of water. However, the partition of ions into POE-surfactant micelles are sometimes discussed on the basis of the complexation of POE chains with cations.<sup>24,25</sup> Such discussions contradict the fact that water-POE (e.g., poly(ethylene glycol)) mixtures can be used for separation of anions rather than cations.<sup>27,28</sup> A  $\zeta$  potential measurement is a useful tool for probing the ionic partition into a micellar nanosphere, and it has allowed us to discuss the binding of ions by ionic and zwitterionic aggregates, where electrostatic interaction basically dominates ionic partition.<sup>16</sup> In contrast, the ionic solvation should play more important roles in the partition of ions into a nonionic micelle. As shown below, a POE-surfactant micelle in general has a negative charge when it is in contact with an electrolyte. The  $\zeta$  potential measurements reveal the extent of a charge excess in the micelle, but cannot explain what causes the charge imbalance; for example, for negative charges, it cannot be explained whether anions are preferably solvated in the micelle or cations are expelled from the micelle.

Ion-transfer voltammetry has been used for the determination of the Gibbs free energy of transfer of an ion between two solvents, and its effectiveness has been well recognized in solution electrochemistry.<sup>29–35</sup> Although this method is basically applied to immiscible solvent systems, the indirect evaluation of ion transfer between miscible solvents is also feasible.<sup>35</sup> If this method can probe the ionic solvation in the hydrophilic layer of the nonionic POE-surfactant micelle, we can discuss what causes the charge imbalance of the micelle. In the present paper, we interpret the charges induced by the partition of ions into a nonionic micelle by means of  $\zeta$  potential and ion-transfer voltammetric measurements. A novel approach without an extrathermodynamic assumption is also devised to determine

\* To whom correspondence should be addressed. E-mail: tokada@chem.titech.ac.jp. Phone and fax +81-3-5734-2612.

the Gibbs free energy of transfer of a single ion from water to the hydrophilic layer of the micelle.

## Experimental Section

**Capillary Electrophoretic Measurements of Micellar Mobility.** A 50  $\mu\text{m}$  id fused silica capillary (GL Science Inc.) was used for the electrophoretic measurements of the  $\zeta$  potential of a micelle. The total length of the capillary was 80.0 cm, and its effective length (i.e., the length between the sample injection end and the detection window) was 68.1 cm. Electrical voltage (10 kV) was applied between both ends of the capillary with a high-voltage electric power unit (Matsusada Precision Inc., HCZE-30P No.25). Solute migration was monitored with an ultraviolet–visible detector (JASCO CE-1570) set to 275 nm. The running buffer contained 50 mM hexaethyleneglycol dodecyl ether (POE6D), an electrolyte (typically 25 mM), and 10 mM  $\text{Na}_2\text{B}_4\text{O}_7$ . A sample solution was injected from the anodic end by siphoning. Acetone and pyrene were added to sample solutions as an electroosmotic marker and a migration marker for micelles, respectively. When running solutions contained  $\text{Br}^-$ , a double-junction electrode was used as the anode to avoid the oxidation of  $\text{Br}^-$ .

**Voltammetric Measurements.** Ion transfer through a microinterface ( $W'$  (or  $W$ )|NB) was voltammetrically measured, where  $W'$ ,  $W$ , and NB denote poly(ethylene glycol) (PEG)-aqueous solutions, aqueous solution, and nitrobenzene solution, respectively. The microinterface was formed using a polyester film with a 50  $\mu\text{m}$  hole according to the literature.<sup>30,31</sup> The electrochemical cell used in this work is summarized as follows:  $\text{Ag}/\text{AgCl} \mid 10 \text{ mM } \text{MgCl}_2(\text{W}) \mid 10 \text{ mM } \text{MgSO}_4(\text{W}) \mid W' \text{ (or } W) \text{ phase} \mid * \text{ NB phase} \mid 1 \text{ mM } [\text{Ph}_3\text{P}=\text{N}=\text{PPh}_3]\text{-BAR}_4(\text{NB}) \mid 10 \text{ mM } \text{Pn}_4\text{NBAr}_4(\text{NB}) \mid 10 \text{ mM } \text{Pn}_4\text{NCl}(\text{W}) \mid \text{AgCl}/\text{Ag}$ , where Pn, Ar, and Ph denote pentyl, 3,5-[bis-(trifluoromethyl)phenyl], and phenyl groups, respectively, and an asterisk refers to the microinterface to be studied. The transfer of an anion was studied with a  $\text{Mg}^{2+}$  salt added to the  $W$  and  $W'$  phases, and similarly that of a cation was measured with a  $\text{SO}_4^{2-}$  or  $\text{Cl}^-$  salt. The aqueous phases contained 10 mM  $\text{MgSO}_4$  as a supporting electrolyte. A  $[\text{Ph}_3\text{P}=\text{N}=\text{PPh}_3]^+$ ,  $\text{Hx}_4\text{N}^+$ , or  $\text{BPh}_4^-$  salt of an ion under study was added to the NB phase, which contained 1 mM  $[\text{Ph}_3\text{P}=\text{N}=\text{PPh}_3]\text{BAR}_4$  as a supporting electrolyte.

Voltamograms at the microinterfaces were recorded by scanning the potential difference,  $E$ , between the  $\text{Ag}/\text{AgCl}$  electrodes with a scanning rate of 0.1  $\text{mV s}^{-1}$ . The potential applied to the  $\text{Ag}/\text{AgCl}$  electrode in  $W'$  (or  $W$ ) versus that in NB was defined as  $E$ . A triangular wave generated by a function generator model WF1943 (NF Electric Instruments) or by a potential generator HB-III (Hokuto Denko) was fed to a potentiostat model HA1010mM1A (Hokuto Denko). Voltamograms were recorded by an XY recorder model F-35CA (Riken Denshi), and the digital data were also acquired by a personal computer via the recorder.

**Chemicals.** POE6D dissolved in water was demineralized with an ion-exchange resin, Amberlite EG-4 (ORGANO), until the conductance of the solution became as low as 0.19  $\mu\text{S cm}^{-1}$ . Reagents used were of the highest grade available. Some salts were purified by recrystallization. Water was purified with a MilliQ system.

**Electrolyte Syntheses.** Sodium Tetrakis[3,5-bis(trifluoromethyl)phenyl]borate ( $\text{NaBAR}_4$ ). In dried diethyl ether, 3,5-bis(trifluoromethyl)bromobenzene was refluxed with metal Mg for 2 h. After it was cooled, the refluxed solution was mixed with dried  $\text{NaBF}_4$ . The solution was refluxed again for 12 h and was

dropwise added to aqueous  $\text{Na}_2\text{CO}_3$  solution after cooling. The ether phase was separated and dried on molecular sieves overnight. After diethyl ether was evaporated, black oily viscous liquid was obtained. The addition of xylene gave deposition, which was filtered and washed with hexane.

*Bis(triphenylphosphine)iminium Tetrakis[3,5-bis(trifluoromethyl)phenyl]-borate* ( $[\text{Ph}_3\text{P}=\text{N}=\text{PPh}_3]\text{BAR}_4$ ). This was deposited by mixing  $[\text{Ph}_3\text{P}=\text{N}=\text{PPh}_3]\text{Br}$  and  $\text{NaBAR}_4$  in ethanol and purified by recrystallization three times.

$[\text{Ph}_3\text{P}=\text{N}=\text{PPh}_3]\text{ClO}_4$ . Perchloric acid was added to  $[\text{Ph}_3\text{P}=\text{N}=\text{PPh}_3]\text{Cl}$  dissolved in ethanol. Deposited  $[\text{Ph}_3\text{P}=\text{N}=\text{PPh}_3]\text{-ClO}_4$  was washed well with water and purified by recrystallization from ethanol twice.

$\text{Pn}_4\text{NBAr}_4$ . The addition of water to the equimolar mixture of  $\text{Pn}_4\text{NBr}$  and  $\text{NaBAR}_4$  in ethanol allowed the deposition of  $\text{Pn}_4\text{NBAr}_4$ , which was washed with methanol.

$\text{Me}_4\text{NBPh}_4$ ,  $\text{KBPh}_4$ ,  $\text{CsBPh}_4$ ,  $\text{Et}_4\text{NBPh}_4$ , *Choline Tetraphenylborate* and *Acetylcholine Tetraphenylborate*. These water-insoluble salts were deposited from aqueous solutions of appropriate water-soluble salts by adding an aqueous sodium tetraphenylborate solution. The redeposition of  $\text{KBPh}_4$  by addition of water to the acetone solution allowed its purification. Other salts were recrystallized from acetone in a usual way.

## Results and Discussion

**Electrophoretic Measurements of Micellar Mobility.** The electrophoretic velocity of a micelle,  $v_{\text{micelle}}$ , is given by

$$v_{\text{micelle}} = v_{\text{app}} - v_{\text{eo}} \quad (1)$$

$$= \frac{L_{\text{eff}}}{t_{\text{app}}} - \frac{L_{\text{eff}}}{t_{\text{eo}}} \quad (2)$$

where  $v_{\text{app}}$  and  $v_{\text{eo}}$  are the apparent velocity of the micelle and the velocity of electroosmosis,  $t_{\text{app}}$  and  $t_{\text{eo}}$  are the migration times of the micelle and electroosmosis, respectively, and  $L_{\text{eff}}$  is the effective length of the capillary. The electrophoretic mobility of the micelle ( $\mu$ ) is given by

$$\mu = \frac{v_{\text{micelle}}}{E} = \frac{L_{\text{eff}}}{E} \left( \frac{1}{t_{\text{app}}} - \frac{1}{t_{\text{eo}}} \right) \quad (3)$$

where  $E$  is the strength of an electric field. The  $\zeta$  potential of the micelle can be calculated by the Henry equation,<sup>36,37</sup>

$$\zeta = \frac{\mu\eta}{\epsilon_0\epsilon_r f(\kappa a)} \quad (4)$$

where  $\kappa$  is a Debye–Hückel shielding parameter,  $a$  is the radius of the micelle, and  $f(\kappa a)$  is the Henry constant given by

$$f(\kappa a) = \frac{2}{3} + \frac{(\kappa a)^2}{24} - \frac{5(\kappa a)^3}{72} - \frac{(\kappa a)^4}{144} + \frac{(\kappa a)^5}{144} + \left\{ \frac{(\kappa a)^4}{24} - \frac{(\kappa a)^6}{144} \right\} \exp(\kappa a) E_1(\kappa a)$$

$$E_1(\kappa a) = -\ln(\kappa a) - 0.5772 + (\kappa a) - 0.2499(\kappa a)^2 + 0.0552(\kappa a)^3 - 0.0098(\kappa a)^4 + 0.0011(\kappa a)^5$$

**TABLE 1: The Results of the  $\mu$ ,  $\zeta$ , and  $N$  of the POE6D Micelles**

electrolyte	$\mu$ $\text{m}^2 \text{s}^{-1} \text{V}^{-1}$	$\zeta$ mV	$N$
$\text{NaClO}_4$	$-5.14 \times 10^{-9} {}^a (1.43 \times 10^{-10})^b$	-9.38	-4.6
$\text{KClO}_4$	$-5.37 \times 10^{-9} (1.79 \times 10^{-10})$	-9.81	-4.8
$\text{Me}_4\text{NClO}_4$	$-5.48 \times 10^{-9} (8.20 \times 10^{-11})$	-10.0	-4.9
$\text{Et}_4\text{NClO}_4$	$-5.02 \times 10^{-9} (1.16 \times 10^{-10})$	-9.17	-4.5
$\text{KCl}$	$-1.09 \times 10^{-9} (8.94 \times 10^{-11})$	-2.00	-0.98
$\text{KBr}$	$-1.13 \times 10^{-9} (1.66 \times 10^{-11})$	-2.07	-1.0
$\text{Me}_4\text{NBr}$	$-1.79 \times 10^{-9} (5.33 \times 10^{-12})$	-3.27	-1.6
$\text{Et}_4\text{NBr}$	$-1.47 \times 10^{-9} (6.80 \times 10^{-11})$	-2.69	-1.3

<sup>a</sup> Negative value means mobility toward the anode. <sup>b</sup> Standard deviation.

The surface electric charge density,  $\sigma$ , can be written as

$$\sigma = \left( \frac{2\epsilon_r \epsilon_0 \kappa k_B T}{e} \right) \sinh \frac{y_0}{2} \times \left[ 1 + \frac{2}{\kappa a \left( \cosh \frac{y_0}{4} \right)^2} + \frac{8 \ln \left( \cosh \frac{y_0}{4} \right)}{(\kappa a)^2 \left( \sinh \frac{y_0}{2} \right)^2} \right]^{1/2} \quad (5)$$

where  $k_B$ ,  $T$ , and  $e$  are the Boltzmann constant, temperature, and the elementary electric charge, respectively, and  $y_0$  is the nondimensional surface potential,

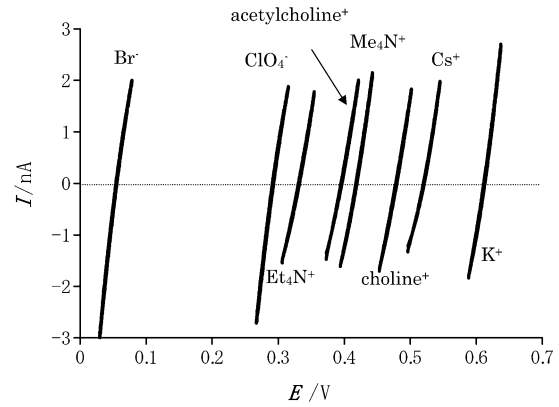
$$y_0 = \frac{e\psi_0}{k_B T} \quad (6)$$

If the shear plane corresponds to the real surface,  $\zeta = \psi_0$ . A charge excess per micelle,  $N$ , is expressed by

$$N = \sigma(4\pi a^2) \frac{1}{e} \quad (7)$$

As discussed below, effects of the electrostatic potential inside the micelle were assumed to be negligible in this paper.

Table 1 lists  $\mu$ ,  $\zeta$ , and  $N$  for POE6D micelles in the presence of various electrolytes (25 mM). A POE6D micelle is thought to be spherical, and its radius is reported to be 3.3 nm according to the literature.<sup>38</sup> The  $\zeta$  potential of the micelle was calculated from  $\mu$  using this radius. Obviously, poorly hydrated anions are partitioned into the micelle better than well hydrated counterparts; that is, the partition of ions becomes more marked in the order of  $\text{Cl}^- < \text{Br}^- < \text{ClO}_4^-$ . In contrast, interestingly, changing cations does not result in clear differences in the mobility or  $\zeta$  potential. These results thus indicate the important involvements of anions in the determination of the partition of ions into the POE nonionic micelle. In addition to the dependence of the  $\zeta$  potential on the type of anions, it should be noted that the  $\zeta$  potential is negative for all of the electrolytes studied here. It is known that POE forms complexes with hard cations, such as  $\text{K}^+$  and  $\text{Rb}^+$ . Although POE6 is so short that its complexation ability is not very high even in appropriate medium, for example methanol, the preferable interaction of POE chains with hard cations is predictable.<sup>26</sup> Nevertheless, the negative  $\zeta$  potential was detected even in the presence of  $\text{KCl}$ , and the interaction of POE with  $\text{K}^+$  is not of crucial importance in the partition of ions into the POE6D micelle. The hydration energies for  $\text{K}^+$  and  $\text{Cl}^-$  are reported to be  $-304$  and  $-347$   $\text{kJ mol}^{-1}$ , respectively. Although it must be difficult to directly compare these values,  $\text{Cl}^-$  is possibly hydrated better than  $\text{K}^+$ . If the transfer of these ions from water into the micelle is

**Figure 1.** Voltammograms for selected ions obtained at the W/NB interface.

accompanied by the dehydration, the larger free energy loss due to the dehydration of  $\text{Cl}^-$  should be compensated by more preferable solvation in the micelle than  $\text{K}^+$ . Thus, though we can qualitatively discuss the results summarized in Table 1 in a similar fashion, it is obvious that the solvation of individual ions should be required for further discussion.

**Ion Transfer Voltammetry.** The standard free energy of transfer of a given ion from the  $\beta$  phase to the  $\alpha$  phase,  $\Delta_\beta^\alpha G^\circ$ , is related to the standard liquid junction potential between these phases,  $\Delta_\alpha^\beta \phi^\circ$ , by the following relation,

$$\Delta_\beta^\alpha G^\circ = zF\Delta_\alpha^\beta \phi^\circ \quad (8)$$

The standard free energy of transfer of an ion from W to W' ( $\Delta_W^{W'} G^\circ$ ) cannot be directly measured because of the miscibility of these phases. However,  $\Delta_W^{W'} G^\circ$  can be indirectly determined if we can measure the standard transfer free energy between NB and W and that between NB and W'.<sup>35</sup>

$$\Delta_W^{W'} G^\circ = \Delta_W^{\text{NB}} G^\circ - \Delta_{W'}^{\text{NB}} G^\circ \quad (9)$$

In the present study, the zero current ion-transfer potential,  $E_{I=0}$ , was measured with a cell illustrated in the Experimental Section. This measurement was carried out for the interface between two immiscible phases containing a common analyte ion. Voltammograms for selected ions obtained at the W/NB interface are depicted in Figure 1. An important feature of the zero current measurements is that the diffusion coefficients are not involved because the entire system is equilibrated.<sup>29,30</sup>

$$E_{I=0} = E^\circ + \frac{RT}{zF} \ln \frac{a_W}{a_{\text{NB}}} = E^\circ + \frac{RT}{zF} \ln \frac{\gamma_W}{\gamma_{\text{NB}}} + \frac{RT}{zF} \ln \frac{c_W}{c_{\text{NB}}} \quad (10)$$

This equation can be written as

$$E_{I=0} = E^{\circ'} + \frac{RT}{zF} \ln \frac{c_W}{c_{\text{NB}}} \quad (11)$$

$E_{I=0}$  is related to  $\Delta_\alpha^\beta \phi^\circ$  by

$$\Delta_{\text{NB}}^W \phi^\circ + \text{const} = E_{I=0} + \frac{RT}{zF} \ln \frac{\gamma_W}{\gamma_{\text{NB}}} \quad (12)$$

where const is the sum of interfacial potentials except the liquid junction potential under study. The zero current potential measured for a monovalent ion should contain the identical const term, if the same experimental system is employed. Thus, the following relation should hold when  $E_{I=0}$  values are measured

for both a cation ( $M^+$ ) and an anion ( $X^-$ ).

$$\begin{aligned}\Delta E_{I=0} &\equiv E_{I=0,M^+} - E_{I=0,X^-} \\ &= \left( \Delta_{NB}^W \phi_{M^+}^o + \text{const} - \frac{RT}{F} \ln \frac{\gamma_{M^+(W)}}{\gamma_{M^+(NB)}} \right) - \\ &\quad \left( \Delta_{NB}^W \phi_{X^-}^o + \text{const} + \frac{RT}{F} \ln \frac{\gamma_{X^-(W)}}{\gamma_{X^-(NB)}} \right) \\ &= \Delta_{NB}^W \phi_{M^+}^o - \Delta_{NB}^W \phi_{X^-}^o - \frac{RT}{F} \ln \left( \frac{\gamma_{M^+(W)}}{\gamma_{M^+(NB)}} \frac{\gamma_{X^-(NB)}}{\gamma_{X^-(W)}} \right) \quad (13)\end{aligned}$$

Eq 13 can then be rewritten as

$$F\Delta E_{I=0} = \Delta_W^{NB} G_{tr,M^+}^o + \Delta_W^{NB} G_{tr,X^-}^o - RT \ln \left( \frac{\gamma_{M^+(W)}}{\gamma_{M^+(NB)}} \frac{\gamma_{X^-(NB)}}{\gamma_{X^-(W)}} \right) \quad (14)$$

A similar equation can be derived when the water phase is replaced by an aqueous PEG solution ( $W'$ ). Thus, we obtain

$$F(\Delta E_{I=0} - \Delta E'_{I=0}) = \Delta_W^{W'} G_{tr,M^+}^o + \Delta_W^{W'} G_{tr,X^-}^o - RT \ln \left( \frac{\gamma_{M^+(W)}}{\gamma_{M^+(W')}} \frac{\gamma_{X^-(W)}}{\gamma_{X^-(W')}} \right)$$

When  $\gamma_{M^+(W)} = \gamma_{M^+(W')}$  and  $\gamma_{X^-(W)} = \gamma_{X^-(W')}$ ,

$$F(\Delta E_{I=0} - \Delta E'_{I=0}) = \Delta_W^{W'} G_{tr,M^+}^o + \Delta_W^{W'} G_{tr,X^-}^o \quad (15)$$

where  $\Delta E'_{I=0}$  is the zero current potential measured with a  $W'/NB$  interface. The validity of the assumption on the activity coefficients is discussed later.

One of the most important issues in the present study is the selection of  $W'$ , which should be a model for the palisade layer of the POE6D micelle. Although an aqueous solution of PEG must be an appropriate model, there are a number of possible choices in the chain length and concentration of PEG. It is known that the hydration number of PEG chains strongly depends on a method used for evaluation.<sup>39–41</sup> Chemical trapping, for example, gave 4.3 (20 °C) and 3.5 (40 °C) for the hydration number per oxyethylene unit in the POE6D micelle,<sup>39</sup> whereas dielectric constant measurements indicated that this number was 10 (10 °C) and 4 (45 °C).<sup>40</sup> Although other methods also gave different numbers, it generally ranges from 2 to 5 at the ambient temperature. In addition, some studies revealed that the hydration number depends on the position along the POE chains as well as the structures of terminal functional groups.

Taking these results into account, we selected several aqueous PEG solutions as model solutions for the palisade layer of the POE6D micelle and measured  $\Delta E'_{I=0}$  for  $Me_4N^+$  and for  $ClO_4^-$  as summarized in Tables 2 and 3. Table 2 shows the effect of the PEG chain length on the  $\Delta E'_{I=0}$  values when the hydration number per oxyethylene group is kept at five. Interestingly, the effect of chain length is not so pronounced that the  $\Delta E'_{I=0}$  value becomes constant when the number of repeating oxyethylene units exceeds two. Tetraethylene glycol (tetraEG) was therefore selected as a model for the palisade layer of the POE6D micelle. Table 3 shows the effects of tetraEG concentration on the  $\Delta E'_{I=0}$  values. The liquid-junction potential at the interface between 10 mM  $MgSO_4$  ( $W$ ) and the  $W'$  phase should be varied with

**TABLE 2:  $\Delta E'_{I=0}$  Measured for  $Me_4N^+$  and for  $ClO_4^-$  with Various PEGs**

PEG <sup>a</sup>	$\Delta E'_{I=0}/mV$
EG	101 (1.8) <sup>b</sup>
diEG	114 (2.0)
triEG	118 (2.8)
tetraEG	118 (2.3)
PEG200	118 (2.9)
PEG300	118 (2.3)
without PEG (water)	127(3.0)

<sup>a</sup> The concentrations of PEG were 41.9% (v/v) for EG, 35.7% (v/v) for diEG, 33.5% (v/v) for triEG, 32.4% (v/v) for tetraEG, 32.1% (v/v) for PEG200, and 31.1% (v/v) for PEG300. These concentrations correspond to five water molecules per oxyethylene unit. <sup>b</sup> Standard deviations in parentheses.

**TABLE 3:  $\Delta E'_{I=0}$  Measured for  $Me_4N^+$  and for  $ClO_4^-$  with Various TetraEG Concentrations**

concentration of tetraEG %	30 (5.6) <sup>a</sup>	32.4 (5.0)	40 (3.6)	50 (2.4)
$\Delta E'_{I=0}/mV$	121	118	116	114

<sup>a</sup> The number of water molecules per oxyethylene unit.

the composition of the latter phase, particularly when the concentration of PEG is high (see the cell shown in the Experimental Section). However, as shown in eq 13, this effect is canceled out, when we discuss  $\Delta E'_{I=0}$  values. The values slightly decrease with increasing tetraEG concentration. This decrease is, however, very small especially when the standard deviation (generally 2–3 mV) of the values reported in this table is taken into account. The aqueous tetraEG solution can thus mimic the hydrophilic layer of the micelle very well, when its concentration is higher than 30% (or the hydration number per oxyethylene unit is less than five). However, we will bear the effect of tetraEG concentration in mind for the following discussions.

As stated above, the activity coefficients of ions in  $W'$  were assumed to be equal to those in  $W$ . An effect of an ionic strength in  $W$  and  $W'$  on  $\Delta E_{I=0} - \Delta E'_{I=0}$  was studied to justify this assumption. For the transfer of  $Me_4N^+$  and  $ClO_4^-$ , the ionic strength did not influence the  $\Delta E_{I=0} - \Delta E'_{I=0}$  values over the range 40–400 mM; the variation of the  $\Delta E_{I=0} - \Delta E'_{I=0}$  values with changing the ionic strength was smaller than 2.1 mV. Hence, the activity coefficients can reasonably be canceled for the derivation of eq 15 at least for monovalent ions, and a special care is not necessary in the present treatments.

**Consistency of Voltammetric Measurements with  $\zeta$  Potential of the POE6D Micelle.** An extrathermodynamic assumption has been employed to separate anionic and cationic contributions involved in various physicochemical values obtained with an electrolyte. Tetraphenylarsonium tetraphenylborate (TATB) hypothesis is one of the most generally applied extrathermodynamic assumptions. This assumption was first utilized to evaluate the Gibbs free energy of transfer of a single ion as well as to cancel the difference in liquid–liquid interface potential between  $W/NB$  and  $W'/NB$ . However, this attempt has been proven unsuccessful; that is, the values determined with this hypothesis always predict positive potentials for the POE6D micelle. Schurhammer and Wipff indicated that the solvation energies of  $Ph_4As^+$  and  $Ph_4B^-$  are not always the same, for example,  $Ph_4As^+$  is more easily transferred from water to dried chloroform than  $Ph_4B^-$ .<sup>42</sup> Our results also suggest the limitation of the TATB hypothesis in this particular instance.

The following approach, in which ion-transfer voltammetry and electrophoresis are cooperatively utilized, has been devised



to overcome the problem noted above. The chemical potential of an ion in a micelle-water system is represented by

$$\mu_{i(W)} = \mu_{i(W)}^{\circ} + RT \ln a_{i(W)} + z_i F \psi_{(W)} \quad (16)$$

$$\mu_{i(M)} = \mu_{i(M)}^{\circ} + RT \ln a_{i(M)} + z_i F \psi_{(M)} \quad (17)$$

where  $\mu_i^{\circ}$ ,  $a_i$ ,  $z_i$  and  $\psi$  are the standard chemical potential, activities, the charge of an ion,  $i$ , and electrostatic potential, respectively; the subscripts, (W) and (M), denote the bulk aqueous solution and the hydrophilic layer of the micelle, respectively. Since  $\mu_{i(W)} = \mu_{i(M)}$  at equilibrium,

$$\mu_{i(W)}^{\circ} - \mu_{i(M)}^{\circ} = RT \ln \frac{a_{i(M)}}{a_{i(W)}} + z_i F (\psi_{(M)} - \psi_{(W)}) \quad (18)$$

The left hand of the above equation can be replaced by the Gibbs free energy of transfer.

$$\mu_{i(W)}^{\circ} - \mu_{i(M)}^{\circ} = -\Delta_{tr,i}^M G^{\circ} \quad (19)$$

where  $\Delta_{tr,i}^M G^{\circ}$  is the standard transfer free energy of  $i$  from water to a micelle. From eqs 18 and 19,

$$\frac{a_{i(M)}}{a_{i(W)}} = \exp \left\{ -\frac{\Delta_{tr,i}^M G^{\circ} + z_i F (\psi_{(M)} - \psi_{(W)})}{RT} \right\} \quad (20)$$

For a 1:1 electrolyte (MX) system,

$$\frac{a_{M^{+}(M)}}{a_{M^{+}(W)}} - \frac{a_{X^{-}(M)}}{a_{X^{-}(W)}} = \exp \left\{ -\frac{\Delta_{tr,M^{+}}^M G^{\circ} + F (\psi_{(M)} - \psi_{(W)})}{RT} \right\} - \exp \left\{ -\frac{\Delta_{tr,X^{-}}^M G^{\circ} - F (\psi_{(M)} - \psi_{(W)})}{RT} \right\} \quad (21)$$

When the volume of the aqueous solution is much larger than that of hydrophilic layers of micelles, and  $\gamma_{M^{+}(W)} = \gamma_{M^{+}(M)}$  and  $\gamma_{X^{-}(W)} = \gamma_{X^{-}(M)}$ , the concentration of the electrolyte ( $c_0$ ) can replace the activity terms. The left side of eq 21 is rewritten as

$$\frac{c_{M^{+}(M)}}{c_0} - \frac{c_{X^{-}(M)}}{c_0} = \frac{(c_{M^{+}(M)} - c_{X^{-}(M)}) V_{POE}}{c_0 V_{POE}} = \frac{N}{c_0 \times V_{POE} \times N_A} \quad (22)$$

where  $N_A$  is the Avogadro constant,  $V_{POE}$  and  $N$  are the volume of hydrophilic layers of a micelle and the charge excess, respectively. As long as the  $W'$  phase represents the palisade layer of the POE6D micelle, the equalities of activity coefficients can be verified by analogy with  $\gamma_{M^{+}(W)} = \gamma_{M^{+}(W')}$  and  $\gamma_{X^{-}(W)} = \gamma_{X^{-}(W')}$ .  $V_{POE}$  is given by

$$V_{POE} = \frac{4}{3} \pi a^3 - \frac{4}{3} \pi (a - d)^3 \quad (23)$$

where  $d$  and  $a$  are the thickness of the hydrophilic layer and the radius of the micelle, respectively. Thus, eq 21 is rewritten as eq 24.

$$\Delta_{tr,M^{+}}^M G^{\circ} = -RT \ln \left[ \exp \left\{ -\frac{\Delta_{tr,X^{-}}^M G^{\circ} - F (\psi_{(M)} - \psi_{(W)})}{RT} \right\} + \frac{N}{c_0 N_A V_{POE}} \right] - F (\psi_{(M)} - \psi_{(W)}) \quad (24)$$

The length of the oxyethylene chain in POE6D depends on its

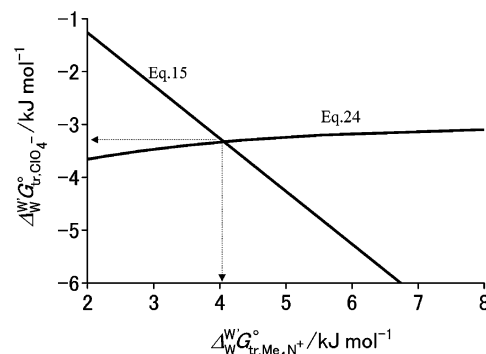


**Figure 2.** Relations between  $\Delta_{tr,Me_4N^+}^{W'} G^{\circ}$  and  $\Delta_{tr,ClO_4^-}^{W'} G^{\circ}$  obtained with eqs 15 and 24:  $W'$ ; 32.4% tetraEG/water. The intersection of these plots gives the  $\Delta_{tr,Me_4N^+}^{W'} G^{\circ}$  and  $\Delta_{tr,ClO_4^-}^{W'} G^{\circ}$  values.

**TABLE 4: Effect of the Thickness of the Hydrophilic Layer ( $d$ ) of the POE6D Micelle on the Gibbs Free Energy of Transfer<sup>a</sup> for  $Me_4N^+$  and  $ClO_4^-$**

$d$ nm	$\Delta_{tr}^{W'} G^{\circ}/kJ mol^{-1}$	
	$Me_4N^+$	$ClO_4^-$
1.5	4.4	-3.5
2.0	4.2	-3.3
2.5	4.1	-3.2
3.0	4.1	-3.2

<sup>a</sup>  $W'$  was 32.4% tetraEG. The radii of the micelle were assumed to be 3.3 nm.

conformation in the micelle. A molecular modeling gave  $d = 2.0$  and  $3.0$  nm for the complete helix structure and the extended zigzag configuration, respectively. The thickness of the palisade layer should thus range from 2.0 to 3.0 nm; the smaller  $d$  values are more consistent with the radius of the POE6D micelle reported to be 3.3 nm.<sup>38</sup> As shown below, the thickness of the palisade layer is not very important for the discussion of the Gibbs free energy of transfer.

The inner potential difference ( $\psi_{(M)} - \psi_{(W)}$ ) cannot be directly related to the  $\zeta$  potential determined by electrophoretic measurements. However, the constant electrostatic potential is not reached inside the micelle, because the double layer thickness in the micelle ( $\sim 2$  nm in a 25 mM solution) almost corresponds to the thickness of the palisade layer. Therefore, the effect of the electrostatic potential inside the micelle is assumed to be negligible in the present work. This effect should be more rigorously discussed using microdroplets of a solvent having well-defined nature. The electrostatic potential of the micelle and a charge excess therein can thus be determined by electrophoretic mobility measurements. We thus have eqs 15 and 24, which represent the relations between  $\Delta_{tr,M^{+}}^{W'} G^{\circ}$  and  $\Delta_{tr,X^{-}}^{W'} G^{\circ}$ . It should be noted that these two equations are independently derived from electrophoretic and ion-transfer voltammetric measurements. Figure 2 illustrates plots based on eqs 15 and 24 for  $Me_4NClO_4$  ( $W' = 32.4\%$  tetraEG). The intersection of these two different curves should give  $\Delta_{tr,Me_4N^+}^{W'} G^{\circ}$  and  $\Delta_{tr,ClO_4^-}^{W'} G^{\circ}$ , which are equal to 4.2 and  $-3.3$  kJ mol<sup>-1</sup>, respectively. Thus, we can determine the Gibbs free energy of transfer of a single ion from water to the palisade layer of the POE6D micelle without the extrathermodynamic assumptions.

As stated above, the thickness of the palisade layer of the micelle,  $d$ , involves some ambiguity. However, this parameter plays a minor role in the determination of  $\Delta_{tr,M^{+}}^{W'} G^{\circ}$  and  $\Delta_{tr,X^{-}}^{W'} G^{\circ}$  on the basis of the present scheme. Table 4 lists  $\Delta_{tr,Me_4N^+}^{W'} G^{\circ}$  and  $\Delta_{tr,ClO_4^-}^{W'} G^{\circ}$  calculated with varying  $d$

**TABLE 5:**  $\Delta_{\text{W}}^{\text{W}}G^{\circ}_{\text{tr}}$  for Several Aqueous TetraEG Solutions

ion	$\Delta_{\text{W}}^{\text{W}}G^{\circ}_{\text{tr}}/\text{kJ mol}^{-1}$		
	30% tetraEG	40% tetraEG	50% tetraEG
$\text{Br}^-$	-1.1	0.4	2.5
$\text{ClO}_4^-$	-3.4	-3.3	-3.3
$\text{Et}_4\text{N}^+$	3.5	3.7	3.5
$\text{Me}_4\text{N}^+$	4.1	4.4	4.5
$\text{Cs}^+$	6.4	7.7	9.5
$\text{K}^+$	13.8	15.7	17.6

**TABLE 6:** The Numbers of Ions in a POE6D Micelle and  $\zeta$  Potentials

	$\zeta$ potential mV			
	calcd at 32.4%	calcd at 40%	calcd at 50%	measd
$\text{KClO}_4$	-11.0	-11.1	-11.2	-9.81
$\text{Me}_4\text{NClO}_4$	-10.0	-10.0	-10.0	-10.0
$\text{Et}_4\text{NClO}_4$	-9.75	-9.76	-9.64	-9.17
$\text{Me}_4\text{NBr}$	-4.33	-2.54	-0.806	-3.27
$\text{Et}_4\text{NBr}$	-4.05	-2.27	-0.505	-2.69

within the possible range 1.5–3.0 nm. Determined  $\Delta_{\text{W}}^{\text{W}}G^{\circ}_{\text{tr}}$  values are almost constant and independent of  $d$ , strongly indicating that the ambiguity of this parameter cannot be a serious disadvantage in the determination of  $\Delta_{\text{W}}^{\text{W}}G^{\circ}_{\text{tr}}$  based on the present approach.

Obviously, once  $\Delta_{\text{W}}^{\text{W}}G^{\circ}_{\text{tr}}$  for a particular ion is determined, the corresponding values for other ions can be also calculated by extending eq 15. The  $\Delta_{\text{W}}^{\text{W}}G^{\circ}_{\text{tr}}$  values of selected ions for aqueous 30, 40, and 50% (v/v) tetraEG solutions were thus determined as listed in Table 5. The  $\Delta_{\text{W}}^{\text{W}}G^{\circ}_{\text{tr}}$  values for  $\text{ClO}_4^-$ ,  $\text{Et}_4\text{N}^+$ , and  $\text{Me}_4\text{N}^+$  are almost the same for 30–50% (v/v) tetraEG, while those for  $\text{Br}^-$ ,  $\text{Cs}^+$ , and  $\text{K}^+$  increases with increasing tetraEG concentration. The latter ions, which are small and relatively well solvated, form large hydration shell in bulk water. The structures of the first hydration shell for these ions formed in the tetraEG solutions must be similar to those in bulk water because of their high electronic densities and hydration ability. However, the contribution from the second hydration shell must be smaller in the tetraEG solutions than in bulk water because the number of available water molecules is highly restricted. The results summarized in Table 5 may imply that such contributions for relatively large ions are not very important.

The  $\zeta$  potentials induced for the POE6D micelle in a given electrolyte should be explained by the  $\Delta_{\text{W}}^{\text{W}}G^{\circ}_{\text{tr}}$  values listed in Table 5. Table 6 compares the experimentally evaluated  $\zeta$  potential of the POE6D micelle with that calculated using the  $\Delta_{\text{W}}^{\text{W}}G^{\circ}_{\text{tr}}$  values of constituent ions. The agreements between these values are better for an electrolyte composed of relatively hydrophobic ions than that containing  $\text{Br}^-$  and  $\text{K}^+$ . Interestingly, the  $\zeta$  potential calculated for a  $\text{Br}^-$  electrolyte from  $\Delta_{\text{W}}^{\text{W}}G^{\circ}_{\text{tr}}$  values is varied with the tetraEG concentration. The best agreement is seen for 40% tetraEG, implying that this concentration best represents the palisade layer of the POE6D micelle. The potential calculated for  $\text{KClO}_4$  is slightly more negative than the measured one irrespective of the concentration of tetraEG in the model solution. This may imply that the model solution is not suitable for  $\text{K}^+$ . Although the interaction of POE with  $\text{K}^+$  must be very weak in aqueous media as noted above, POE6 may more strongly interact with  $\text{K}^+$  than tetraEG. The concentration of  $\text{K}^+$  in the micelle is thus slightly higher than that predicted from the  $\Delta_{\text{W}}^{\text{W}}G^{\circ}_{\text{tr}}$  value for  $\text{K}^+$  determined with aqueous tetraEG as a model solvent.

## Conclusions

As far as the ion transfer from water to aqueous PEG solutions is concerned, a cooperative approach by electrophoresis and ion-transfer voltammetry has proven to be effective and does not require any extrathermodynamic assumptions. Another important finding of the present work is that a large and poorly solvated anion such as  $\text{ClO}_4^-$  is likely to be accumulated in the hydrophilic layer of polyoxyethylated micelles, whereas most of the cations are expelled from the micelles. Although this must be related to the nature of hydration of ions, the molecular details have not been elucidated. Similar phenomenon is known for example in ion-exchange selectivity; the hydration of anions is more selectively recognized by ion-exchangers than that of cations. A difference in  $\Delta_{\text{W}}^{\text{W}}G^{\circ}_{\text{tr}}$  between  $\text{ClO}_4^-$  and  $\text{Me}_4\text{N}^+$  is 7 kJ mol $^{-1}$ , which is no more than ca. 3% of their individual hydration energies. Therefore, the structural origin of this subtle difference may come from the hydration shell far apart from an ion under discussion. To reveal these aspects, molecular dynamic simulations and direct structural analyses by X-ray absorption spectrometry are now in progress in our laboratory.

**Acknowledgment.** We gratefully appreciate invaluable suggestions on the voltammetric measurements as well as gifts of polyester films and  $\text{Ph}_4\text{AsBPh}_4$  by Professors S.Kihara and K.Maeda, Kyoto Institute of Technology. This work has been supported in part by a Grant-in-Aid for Scientific Research from The Japan Society for the Promotion of Science.

## References and Notes

- (1) Liu, Y.; Wang, Q.; Zhang, L.; Wu, T. *Langmuir* **2005**, *21*, 12025.
- (2) Liu, Y.; Wang, Q.; Wu, T.; Zhang, L. *J. Chem. Phys.* **2005**, *123*, 234701/1.
- (3) Okazaki, M.; Toriyama, K. *J. Phys. Chem. B* **2005**, *109*, 13180.
- (4) Takahara, S.; Sumiyama, N.; Kittaka, S.; Yamaguchi, T.; Bellissent-Funel, M.-C. *J. Phys. Chem. B* **2005**, *109*, 11231.
- (5) Corsaro, C.; Crupi, V.; Longo, F.; Majolino, D.; Venuti, V.; Wanderlingh, U. *Phys. Rev. E: Stat. Phys., Plasmas, Fluids, Relat. Interdiscip. Top.* **2005**, *72*, 061504/1.
- (6) Shirono, K.; Daiguji, H. *Chem. Phys. Lett.* **2006**, *417*, 251.
- (7) Crupi, V.; Longo, F.; Majolino, D.; Venuti, V. *J. Chem. Phys.* **2005**, *123*, 154702/1.
- (8) Corsaro, C.; Crupi, V.; Majolino, D.; Migliardo, P.; Venuti, V.; Wanderlingh, U.; Mizota, T.; Telling, M. *Mol. Phys.* **2006**, *104*, 587.
- (9) Ohkubo, T.; Hattori, Y.; Kanoh, H.; Konishi, T.; Fujikawa, T.; Kaneko, K. *J. Phys. Chem. B* **2003**, *107*, 13616.
- (10) Buchner, R.; Baar, C.; Fernandez, P.; Schroedle, S.; Kunz, W. *J. Mol. Liq.* **2005**, *118*, 179.
- (11) Hunt, N. T.; Jaye, A. A.; Meech, S. R. *Chem. Phys. Lett.* **2005**, *416*, 89.
- (12) Messaoud, T.; Duplatre, G.; Michels, B.; Waton, G. *J. Phys. Chem. B* **2004**, *108*, 13137.
- (13) Shi, Z.; Peterson, R. W.; Wand, A. J. *Langmuir* **2005**, *21*, 10632.
- (14) Buchner, R.; Baar, C.; Fernandez, P.; Schroedle, S.; Kunz, W. *J. Mol. Liq.* **2005**, *118*, 179.
- (15) Mahajan, R. K.; Kaur, N.; Bakshi, M. S. *Colloids Surfaces A* **2005**, *255*, 33.
- (16) Iso, K.; Okada, T. *Langmuir* **2000**, *16*, 9199.
- (17) Harada M.; Okada, T. *Langmuir* **2004**, *20*, 30.
- (18) Harada M.; Okada, T.; Watanabe, I. *J. Phys. Chem. B* **2003**, *107*, 2275.
- (19) Wittek, M.; Möller, G.; Johnson, M. J.; Majda, M. *Anal. Chem.* **2001**, *73*, 870.
- (20) Johnson, M. J.; Majmudar, C.; Skolimowski, J. J.; Majda, M. *J. Phys. Chem. B* **2001**, *105*, 9002.
- (21) Kuhn, H.; Rehage, H. *J. Phys. Chem. B* **1999**, *103*, 8493.
- (22) Lu, J. R.; Thomas, R. K.; Binks, B. P.; Crichton, D.; Fletcher, P. D. I.; McNab, J. R.; Penfold, J. *J. Phys. Chem. B* **1998**, *102*, 5785.
- (23) Green, S. R.; Su, T. J.; Lu, J. R.; Penfold, J. *J. Phys. Chem. B* **2000**, *104*, 1507.
- (24) Hagerstrand, H.; Bobacka, J.; Bobrowska-Hagerstrand, M.; Kralj-Iglic, V.; Fosnaric, M.; Iglic, A. *Cellular Mol. Biol. Lett.* **2001**, *6*, 161.
- (25) Siew, D. C. W.; Cooney, R. P.; Taylor, M. J. *Appl. Spectrosc.* **1993**, *47*, 1784.
- (26) Okada, T. *Macromolecules* **1990**, *23*, 4216.

- (27) Ishii, K.; Tanaka, Y.; Hata, K.; Goto, M.; Saitoh, K.; Minamisawa, H.; Shibukawa, M. *Bunseki Kagaku* **2004**, *53*, 911.
- (28) Okada, T. *Anal. Chem.* **1992**, *64*, 2138.
- (29) Yoshida, Y.; Matsui, M.; Maeda, K.; Kihara, S. *Anal. Chim. Acta* **1998**, *374*, 269.
- (30) Ohde, H.; Uehara, A.; Yoshida, Y.; Maeda, K.; Kihara, S. *J. Electroanal. Chem.* **2001**, *496*, 110.
- (31) Beriet, C.; Girault, H. H. *J. Electroanal. Chem.* **1998**, *444*, 219.
- (32) Katano, H.; Murayama, Y.; Tatsumi, H. *Anal. Sci.* **2004**, *20*, 553.
- (33) Kakiuchi, T.; Tsujioka, N. *Electrochem. Commun.* **2003**, *5*, 253.
- (34) Osakai, T.; Ogawa, H.; Ozeki, T.; Girault, H. H. *J. Phys. Chem. B* **2003**, *107*, 9829.
- (35) Suzuki, M. *J. Electroanal. Chem.* **1994**, *372*, 39.
- (36) Ohshima, H. *J. Colloid Interface Sci.* **1996**, *180*, 299.
- (37) Ohshima, H. *J. Colloid Interface Sci.* **1994**, *168*, 269.
- (38) Zulauf, M.; Weckström, K.; Hayter, J. B.; Degiorgio, V.; Corti, M. *J. Phys. Chem.* **1985**, *89*, 3411.
- (39) Romsted, L. S.; Yao, J. *Langmuir* **1996**, *12*, 2425.
- (40) Briganti, G.; Bonincontro, A. *J. Non-Cryst. Solids* **1998**, *235*, 704.
- (41) Briganti, G.; D'Arrigo, G.; Maccarini, M. *J. Phys. Chem. B* **2004**, *108*, 4039 and references therein.
- (42) Schurhammer, R.; Wipff, G. *J. Phys. Chem. A* **2000**, *104*, 11159.